World Journal of Applied Physics
2022; 17(1): 1-10
http://www.sciencepublishinggroup.com/j/wjap
doi: 10.11648/j.wjap.20220701.11
ISSN: 2637-5990 (Print); ISSN: 2637-6008 (Online)

The Study of Diluted Magnetic Semiconductor: The Case of Manganese Doped Gallium Nitride

Merawi Tilahun Tegegne

Department of Physics, Kebridhar University, Qorahay, Ethiopia

Email address:
merawi3016@gmail.com

To cite this article:
Merawi Tilahun Tegegne. The Study of Diluted Magnetic Semiconductor: The Case of Manganese Doped Gallium Nitride. *World Journal of Applied Physics*. Vol. 7, No. 1, 2022, pp. 1-10. doi: 10.11648/j.wjap.20220701.11

Received: January 16, 2021; **Accepted**: April 21, 2021; **Published**: February 16, 2022

Abstract: The diluted magnetic semiconductor, (Ga, Mn) N has recently attracted intense research interest for the purpose of spintronics application. The material is believed to circumvent the difficulty of combining data processing and mass storage facilities in a single crystal besides solving non-volatility problems. The concentration x, of Mn that substitutes for a fraction of Ga in the compound is thought to contribute a large concentration of magnetic moments and holes. The material studied is focused on dilute magnetic semiconductors (DMS) like $Ga_{1-X}Mn_XN$ that play a key role in semiconductor spintronics. Due to their ferromagnetic properties they can be used in magnetic sensors and as spin injectors. The basic problems for applications are, however, the relatively low Curie temperatures of these systems. Therefore, we focus on the understanding of the magnetic properties and on a reliable calculation of Curie temperatures from first principles. We have developed a theoretical framework for calculating critical temperatures by combining first principles calculations and in terms of the Ruderman–Kittel–Kasuya–Yosida quantum spin model in Green's function approach. Magnetic properties of the group-III nitride semiconductors are introduced here with basic material parameters (temperature, concentration, heat capacity, etc. Temperature dependencies of the spin wave specific heat, inverse magnetic susceptibility and reduced magnetization are determined. Therefore, the dependence of the Neel temperature on the manganese ion concentration is linear thus for our calculation the highest Neel temperature obtained T=146.3k within the concentration of 0.2.

Keywords: Diluted Magnetic Semiconductor, Spintronics, Manganese Doped Galium Nitride

1. Introduction

Background and Justification

In recent years, considerable work has been devoted to the study of diluted magnetic semiconductors. [1] Semiconductor physics and magnetism are established subfields of condensed-matter physics that continue to reveal a rich variety of unusual phenomena, often in new types of solid-state materials. [2]. Magnetic orders when it is present, has a large impact on other material properties including transport and optical properties. [3] In both semiconductor and magnetic cases, sophisticated and economically important technologies have been developed to exploit the unique electronic properties mainly for information storage and retrieval in the case of magnetism. The realization of materials that combine semiconducting behavior with robust magnetism has long been a dream of material physists [4]. As technology advances, the number of semiconductors that are used in technology steadily increases. Indeed many innovations have arisen as a result of using new materials and their heterostructures. Thus while silicon, gallium arsenide and indium phosphide have been most widely used, other materials like indium arsenide (InAs), indium nitride (InN), gallium nitride (GaN), zinc oxide (ZnO) etc., are finding important uses as well. It is important to recognize that the ability to examine fundamental physics issues and to use semiconductors in state of the art device technologies depends critically on the purity and perfection of the semiconductor crystal [5]. Transition metal doped GaN finds applications in emerging fields of semiconductor spin transfer electronics (spintronics) which exploit the spin of charge carriers in semiconductors [6]. Based on this concept, some new class of devices available are spin transistors operating at very low powers for mobile applications, optical emitters with encoded information through their polarized light output, fast non-volatile semiconductor memory and integrated

magnetic/electronic/photonic devices. The successful fabrication of the blue light III-IV nitride semiconductor laser was demonstrated [7].

Optical measurements, in connection with a theoretical analysis of the spectroscopic data; provide a very useful tool to analyze impurities in wide-gap semiconductors. Here, we will concentrate on GaN: Mn in zinc-blende structure. GaN in a cubic (zinc-blende) phase can be grown epitaxially on cubic SiC or GaAs. It exhibits a number of very appealing properties for device applications: It has a smaller band gap than the wurtzite phase (by 0.2 eV), it can be easily cleaved, and it has a higher saturated drift velocity [8].

Among all III-nitride semiconductors, gallium nitride (GaN) possesses several remarkable physical properties that make them particularly attractive for reliable solid state device applications. It is a wide band gap (3.4 eV) material having low dielectric constants with high thermal conductivity pathways. It exhibit fairly high bond strengths and very high melting temperatures [6].

The low solubility of Mn in III-V semiconductors was the main barrier to fabrication and it has only recently become possible to grow such materials using low-temperature molecular beam [4]. Ferromagnetic semiconductors within TM elements have great impact and potential for realization of the semiconductor spintronics in the next generation of high-speed, high-density and low power electronics [9].

The electrons and holes are thermally activated and in a temperature range, in which the charged carriers contributed by the impurities dominate, the semiconductor is said to be in the extrinsic temperature range, otherwise it is said to be intrinsic. Over a certain temperature range, donors can add electrons to the conduction band (and acceptors can add holes to the valence band) as temperature is increased. This can cause the electrical resistivity to decrease with increasing temperature giving a negative coefficient of resistance as cited by [10, 4].

Semiconductors have attracted extraordinary interest as the active elements in a wide range of devices including diodes, transistors, logic elements, single-electron transistors, optoelectronic devices, spintronics and sensors [11].

Essentially all of these devices are based on semiconductor structures which provided the stages for exploring questions of fundamental physics. As technology advances, the number of semiconductors that are used in technology steadily increases. Indeed many innovations have arisen as a result of using new materials and their heterostructures. Thus while silicon, gallium arsenide and indium phosphide have been most widely used, other materials like indium arsenide (InAs), indium nitride (InN), gallium nitride (GaN), zinc oxide (ZnO) etc., are finding important uses as well. It is important to recognize that the ability to examine fundamental physics issues and to use semiconductors in state of the art device technologies depends critically on the purity and perfection of the semiconductor crystal [12].

Among all III-nitride semiconductors, gallium nitride (GaN) possesses several remarkable physical properties that make them particularly attractive for reliable solid state device applications. It is a wide band gap (3.4 eV) material having low dielectric constants with high thermal conductivity pathways. It exhibit fairly high bond strengths and very high melting temperatures. The large bond strengths could possibly inhibit dislocation motion and improve reliability in comparison to other II-VI and III-V materials. In addition, the nitrides resist chemical etching, tolerate radiations and therefore, allow GaN-based devices to be operated in harsh environments. GaN is also a suitable candidate for spintronics application as the mature process technology makes it easy for doping magnetic elements into its matrix to induce spin polarization [13].

The GaN based p-n junction LED emission wavelengths were in the range of 370-390 nm, together with deep level emission at 550 nm. There are two basic options. The first method would be colour mixing through integration of red, blue and green LEDs in the same package. The second is colour conversion through the use of a phosphor or organic dye inside the package to convert the blue light from a GaN based LED into white light [12]. Traffic lights using InGaN/AlGaN blue-green LEDs promise to save vast amounts of energy, since their electrical power consumption is only 12 % of that of the present incandescent bulb traffic lights and have extremely long lifetime (>106 h) [14].

There is also a large potential market of GaN in projection displays, where LEDs with the three primary colours would replace the existing liquid crystal modulation system. The high output power of GaN based LEDs and fast off/on times should also have advantages for improved printer technology with higher resolution than existing systems based on infrared lasers [15]. In underwater military systems, GaN lasers may have applications for communications because of a transmission pass band in water between 450 and 550 nm. In the AlGaN system, by varying the Al concentration we can tune the band gaps from 3.4 eV to 6.2 eV. This results in the fabrication of solar-blind UV detectors. UV detectors have a variety of military and civil applications and high temperature sensors are desirable under extreme conditions like inside jet engines.

It also find place in space applications as it is not affected by harmful radiations due to shorter < 280nm wavelength detection limit. There is an increasing interest in the use of compound semiconductors for several high power/high temperature solid state devices for applications in power electronics, control and distribution circuits. While silicon and to a much lesser extent GaAs have been used for power devices, emerging GaN and SiC have significant advantages because of wider band gaps (higher operating temperature), larger breakdown voltages (higher operating voltage), higher electron saturated drift velocity (higher operating current) and better thermal conductivity (higher power density).

Transition metal doped GaN finds applications in emerging fields of semiconductor spin transfer electronics (spintronics) which exploit the spin of charge carriers in semiconductors [16].

2. Material and Method

In this work we have been used the first principles

calculations and in terms of the Ruderman–Kittel–Kasuya–Yosida quantum spin model in Green's function approach to investigated on the dependence of the Neel temperature on the manganese ion concentration, the temperature dependencies of the spin-wave specific heat and reduced magnetization and magnetic properties of transition metal (manganese) doped gallium nitride (GaN) based on first principle calculation method using the Ruderman–Kittel–Kasuya–Yosida quantum spin model in Green's function approach and also we would be employ computational methods using Mat lab program by developing suitable computer codes for studying different properties of transition metal doped (manganese) gallium nitride and we would be developed Mat lab code for our master equation to generate data and the graph in different legends.

2.1. Green's Function Approach to the RKKY Model

The researcher used the standard spin RKKY Hamiltonian model to determine coexistence of ferromagnetic and antiferromagnetic interactions. Hamiltonian thus allows a coexistence of ferromagnetic and antiferromagnetic interactions in the system [8].

The Hamiltonian used to describe the system consists of quantized magnon- magnon interaction energies written as

$$H = \frac{-1}{2}\sum J_{ij}\,\hat{\mathrm{S}}_i\hat{\mathrm{S}}_j \tag{1}$$

Where J_{ij} is the RKKY effective spin exchange interaction between local spin $\hat{S}i$ and $\hat{S}\,j$, ($\hat{\mathrm{S}}_i$and $\hat{\mathrm{S}}_j$ are both quantum spin operators), formula

$$J_{ij} = J_{pd}^2\, m^k\, \frac{K_F^4}{2\pi^3\hbar^2}\, F\left(2K_F R_{ij}\right) \tag{2}$$

where F (x) is an oscillating function defined by the oscillatory nature of the RKKY.

$$F(x) = \frac{[\mathrm{X}\cos(\mathrm{x}) - \sin(\mathrm{x})]}{\mathrm{X}^4}$$

The coupling constant J_{pd} in equation (2) is the local coupling of the itinerant spin to the local magnetic moment, m^* is the effective mass of the carrier, K_F is the Fermi wave vector … under free electron gas approximation) *Rij* is the distance between local magnetic moments at R_i and R_j. Here, the magnetic atoms are distributed randomly in the full lattice of the undoped semiconductor. The prime for the summation in equation (1) means that the summation is done only over the sites occupied by magnetic impurities. Hence, we use Green's function approach (1) to treat the model equation (1) In this scheme one uses a double-time Green's function $\ll \hat{A}(t); \hat{B}(t') \gg$ this satisfies the following equation of motion:

$$i\hbar\frac{d}{dt} \ll \hat{A}(t); \hat{B}(t') \gg = \delta(t-t') \; < \left[\hat{A}\,(t), \hat{B}(t') > + \ll \left[\hat{A}(t), \hat{\mathrm{H}}\right]\right]; \hat{B}(t') \tag{3}$$

This approach proves successful for various Heisenberg spin models on regular lattices. Usually, one needs more than one Green's function when spin S is larger than for our random spin system we construct double-time spin Green's functions between 1/2 spin operators at two magnetic sites *Ri* and Rj.

$$G^n_{ij(t,t')=} \ll \hat{\mathrm{S}}_i^+(t); \left(\hat{\mathrm{S}}_j^-(t')\right)^{n-1} \gg \tag{4}$$

Where' n' takes 1, 2, 3... 2S. as a rule, we needs 2S independent Green's functions for spin S. They can be expressed as

$$G^n_{ij}(t,t') = \frac{1}{2\pi\hbar}\int G^n_{ij}\,(\omega)e^{-\frac{i\omega(t-t')}{\hbar}}d\omega$$

2.2. The Green's Function Formalism

The Green functions play the most important part in the field theoretical treatment of the many body problems, and are especially useful for summing over the restricted classes of perturbation theory of diagrams, and also are very power full when combined with spectral representations. And also they are flexible enough to describe the effects of retarded interactions and all quantities of physical interest like thermodynamic properties can be derived from them. There are different types of Green functions, or propagators: one particle, two- particle... n particles, advanced, retard the Curie temperature itself is a critical point, where the magnetic susceptibility is theoretically infinite and, although there is no net magnetization, domain-like spin correlations fluctuate at all length scales d, zero temperature, finite temperature, real-time, imaginary time (2)

$$G_{kk'}(t-t') = \ll b_k(t); b^+_{k'}(t') \gg = -i\theta(t-t') - < [b_k(t); b^+_k(t')] > \tag{5}$$

Where $\ll \cdots \gg is$ the abbreviated notations for the Fourier transform of the corresponding Green's function and <... > denotes averaging over a ground canonical ensemble. This is appropriate since the number of particles is not constant and $\theta(t)$ is the step function. We note from (2) and (4) that $G_{kk'}(t-t') \neq 0$ when $t' < t, G_{kk'}(t-t') = 0$ when $t' > t$, and $G_{kk'}(t-t')$ is not defined when $t' = t$, because of the discontinuity of $\theta(t)$ at t=0. One important property of $G_{kk'}(t-t')$ is that it depends only on the difference $(t-t')$ in the case of statistical equilibrium.

$$\theta(t-t') = 1\; if\; t > t'\; and\; \theta(t-t') = 0\; if\; t < t' \tag{6}$$

$$G_{kk'}(t-t') = \ll b_k(t), b^+_{k'} \gg = \ll b_k, b^+_{k'} \gg \tag{7}$$

In order to obtain equation of motion we differentiate equation (1) With respect to t and multiplying both sides of (3) by i.

$$i\frac{d}{dt}G_{kk'}(t-t') = i\frac{d}{dt} \ll b_k(t), b^+_{k'}(t') \gg = \; \delta(t-t') < [b_k(t), b^+_{k'}(t')] > + \ll [b_k(t), H], b^+_{k'}(t') \gg$$

To solve equation (3) it is convenient to work with the Fourier transformation of this equation.

Now let $G_{kk\prime}(\omega)$ be the Fourier transform of $G_{kk\prime}(t-t')$ such that

$$G_{kk\prime}(t-t') = \int G_{kk\prime}(\omega)e^{-i\omega(t-t\prime)}d\omega \quad (8)$$

And

$$G_{kk\prime}(t-t') = \int G_{kk\prime}(t-t')e^{-i\omega(t-t\prime)}d(t-t') \quad (9)$$

In addition, the delta function can be defined as

$$\delta(t-t') = \int e^{i\omega(t-t')}d\omega \quad (10)$$

Using equation (5), (6) and (7) in equation 4 we have got,

$$\omega G_{kk\prime}(\omega) = [b_k(t), b_{k\prime}(t')] > \omega + \ll [b_k(t), H]; b_{k\prime}(t') \gg \omega \quad (11)$$

Where $i\frac{d}{dt}b_k(t) = [b_k(t), H]$ And $H =< H^{magnon} >= \omega_k < b_k^+; b_k >$

The commuting and anti-commuting relation for the two operators is also given by:

$$[b_k b_{k\prime}] = b_k b_{k\prime} - \eta b_k b_{k\prime}.$$

Where η=1for Boson operators, and $\eta = -1$ for fermions operators. That is

$$[\, b_k b_{k\prime}^+] = b_{k\sigma} b_{k\prime\sigma}^+ - b_{k'\sigma}^+ b_{k\sigma} \quad (12)$$

For two boson operators:

$$b_{k\sigma} b_{k'\sigma'} = 0 \quad (13)$$

For two fermions operator:

$$b_{k'\sigma'} = b_{k\sigma} b_{k'\sigma'}^+ + b_{k'\sigma'}^+ b_k = \delta_{kk'}\delta_{\sigma\sigma'} \quad (14)$$

$$\{b_{k\sigma}, b_{k'\sigma'}\} = \{b_{k\sigma}^{+i} b_{k'\sigma'}^{+i}\} = 0 \quad (15)$$

The correlation function $< b_{k'}(t), b_k(t) >$ is related to the analytic property of Green functions by $< b_{k'}^{+i}(t) b_k(t) >= i\, lim_{\sigma\to 0}\, i\frac{\int_{-\infty}^{\infty}\left[\ll b_k, b_{k'}^+ \gg \omega + i\delta - \ll b_k b_{k'}^+ \gg -i\delta\right] e^{\omega(t-t')}d\omega dt}{e^{\beta\omega}-1}$

$$i\frac{d}{dt}b_k = \left[b_k, \sum_k \omega_k^+ b_{k'}^+, b_k\right]$$

$$= \sum \omega\left[b_k, b_{k'}^{+i} b_k\right]$$

$$= \sum_{kk'} \omega_k \left[b_k, b_{k'}^{+i} b_k\right] b_k + \sum_{kk'} \omega_k\, b_{k'}^{+i}[b_k b_k]$$

$$= \sum_{kk'} \omega_k b_k \delta_{kk'} + 0 = \omega_k b_k, k = k'$$

Taking the Fourier transformation(2.6), we get

$$\omega G_{kk'} = \frac{\delta_{kk'}}{2\pi} + \ll [b_k, H], b_{k'}^+ \gg \omega \quad (16)$$

Where $[b_k, H]$ is the commutation relation of $b_k\, with$ the magnon Hamiltonian, where $[b_k, H^{magnon}] = \omega_k b_k\, and for\, k = k', \delta_{kk'} = 1$

These give

$$\omega G_{kk}(\omega) = \frac{1}{2\pi} + \ll \omega_k b_k, b_{k'}^+ \gg \omega \quad (17)$$

Where $\ll \omega_k b_k, b_{k'}^+ \gg \omega = \omega_k \ll b_k, b_k^+ \gg = \omega G_{kk}(\omega)$ from which we obtain

$$(\omega = \omega_k) G_{kk}(\omega) = \frac{1}{2\pi}, G_{kk}(\omega) = \frac{1}{2\pi(\omega-\omega_k)} \quad (18)$$

Poles of the Green function are given by $(\omega - \omega_k)$ from which we find despersion. Again considering equation(7) and taking t=t' equal time correlation gives the number operators;

$$\ll b_k, b_k^+ \gg + i\delta = \frac{1}{2\pi(\omega+i\delta)-\omega_k} = \frac{1}{2\omega}\left[\frac{P}{(\omega-\omega_K)} + i\delta\omega(\omega-\omega_k)\right] \quad (19)$$

$$\ll b_k, b_k^+ \gg - i\delta = \frac{1}{2\pi(\omega-i\delta)-\omega_k} = \frac{1}{2\omega}\left[\frac{P}{(\omega-\omega_K)} + i\delta\omega(\omega-\omega_k)\right] \quad (20)$$

Where P is the principal part of the integral…finally;

$< b_k b_k >= \lim_{\delta\to 0} i\int \delta(\omega-\omega_k)\frac{d\omega}{e^{\beta\omega}-1}$ This can be expressed as

$$n_k = \frac{1}{e^{\beta\omega}-1} \quad (21)$$

Where $n_k =< b_k b_k >$ is the number of magnons in state k.

2.3. Magnon Distributions Function

A magnon is a quantized spin wave [17]. The ground state of a simple ferromagnet has all spins Parallel. At long wave lengths ka << 1 so that, the frequency of magnon ω_k is proportional to k^2; In the same limit the frequency of a phonon is proportional to k.

The quantization of spin waves proceeds exactly as for photons and phonons. The energy of a mode of frequency with $\omega_k\, n_k$ magnons can also be equated to,

$$E_k = \left(n + \frac{1}{2}\right)\hbar\omega_k \quad (22)$$

The excitation of magnon of corresponds to the reversal of one spin $\frac{1}{2}$ equation (12) is the Bose-Einstien distribution that magnons also obey. The total number of magnons in all modes excited at temprature T can be caculated as:

$$\sum_k < n_k >= \int D(\omega)n(\omega)d\omega \quad (23)$$

Where $D(\omega)$ is the number of magnon modes per unit frequency range. The integral is taken over the allowed range of k, which is the first Brillouin zone. At sufficiently low

temperature we may carry the integral between 0 and ∞ because $< n(\omega) > \rightarrow 0$ exponentially as $\rightarrow \infty$.

Magnons have a single polarization for each value of k [12].

In three dimensions the number of modes of wave vector less than k is $\left(\frac{1}{2\pi}\right)^3 (4\pi k^3)$ per unit volume, hence the number of magnons with frequency in $d\omega$ at ω is:

$$\left(\frac{1}{2\pi}\right)^3 (4\pi k^2) \frac{dk}{d\omega} \tag{24}$$

Under this assumption, the magnon part of the Hamiltonian can be written like a harmonic oscillator or phonon type Hamiltonian:

$$\langle H^{magnon} \rangle = \sum_k \hbar_k \omega_k \tag{25}$$

Where is the average number of magnons in state k and $\omega_k = 2xJSa^2k^2$ is the long wave length magnon dispersion. substituting ω_k in to equation (25), for ω_k we get

$$< b_k^+ b_k >= \frac{1}{e^{\frac{2xJSa^2k^2}{k_BT}} - 1} \tag{26}$$

$$\sum_k < n_k >= \frac{1}{2\pi^3} \int_0^\infty \frac{4\pi k^2 dk}{e^{\frac{2xJSa^2k^2}{k_BT}} - 1} \tag{27}$$

$$\sum_k < n_{k>} = \frac{1}{2\pi^2} \int_0^\infty \frac{k^2 dk}{e^{\frac{2xJSa^2k^2}{k_BT}} - 1} \tag{28}$$

$let\ y = \frac{2xJSa^2k^2}{k_BT}$ and dy $= \frac{4xJSa^2k^2dk}{k_BT}$ solving k,

$$k = \left(\frac{k_bT}{2XJSa^2}\right)^{\frac{1}{2}} y^{\frac{1}{2}} \tag{29}$$

and

$$k^2dk = \left(\frac{k_bT}{2XJSa^2}\right)^{\frac{1}{2}} \frac{y^{\frac{1}{2}}}{2} \tag{30}$$

Substituting equation (2.21) in to (2.19), we get

$$\sum_k n_k = \frac{1}{2\pi^2} \int_0^\infty \left(\frac{k_BT}{2XJSa^2}\right)^{\frac{3}{2}} \int_0^\infty \frac{y^{\frac{1}{2}}}{e^y - 1} \tag{31}$$

Where the integratio

$$\int_0^\infty \frac{y^{\frac{1}{2}}}{e^y - 1} = 2.3174 \tag{32}$$

$$hence\ \sum_k n_k = (2.3174) \left(\frac{k_BT}{2XJSa^2}\right)^{\frac{3}{2}} \tag{33}$$

$$\sum_k n_k = (0.0587) \left(\frac{k_BT}{2XJSa^2}\right)^{\frac{3}{2}} \tag{34}$$

Where eqution (25) gives us the number of reversed spins given by the ensemble average of the spin wave occupancy numbers.

The average magnons excitation energy at low temprature is given by: $\langle H^{magnon} \rangle = \sum_k \langle n_k \rangle \omega_k$.

2.3.1. Magnon Heat Capacity in Ferromagnetism

Magnons are other important types of energy excitation and they occur in magnetically ordered solids (3). The internal energy of unit volume of magnon gas in thermal equilibrium at a temperature T_i neglecting magnon-magnon interaction, at very low external field and considering $ka \ll 1\ is\ given\ by$:

$$U = \sum_k \omega_K \langle n_k \rangle_T = \sum_K \frac{\omega_K}{e^{\beta\omega} - 1} \tag{35}$$

$$\text{taking } \omega_k = 2xJSa^2k^2 \tag{36}$$

$$U = \frac{1}{(2\pi)^3} \int_0^\infty \frac{\omega_K 4\omega K^2 dk}{\frac{2xJSa^2k^2}{K_BT}} \tag{37}$$

Again from equation (3.16) $d\omega_k = 2xJSa^2(2k)dk$ and $\text{dk}^2 = \frac{\omega_K}{2xJSa^2}$

We get $\text{dk}^2 = \frac{1}{(8xJSa^2)} \omega_K^{\frac{1}{2}} d\omega_K$

$$U = \frac{1}{(8xJSa^2)^{\frac{1}{2}}} \frac{1}{4\pi^2} \int_0^\infty \frac{\omega_K^{\frac{3}{2}}}{\frac{2xJSa^2k^2}{e^{\beta\omega} - 1}} \tag{38}$$

Let

$y = \frac{\omega_K}{k_B} T$ and $\frac{d\omega_K}{k_BT} = dy \Rightarrow dyk_BT = d\omega_K\ and\ k_BT = \frac{d\omega_K}{dy}$

$$\text{Where } \frac{1}{4\pi^2} \int_0^\infty \frac{y^{\frac{3}{2}}}{e^y - 1} = 0.0456 \text{ then} \tag{39}$$

$$U = 0.0456 \left(\frac{1}{2xJSa^2}\right)^{\frac{3}{2}} k_B^{\frac{5}{2}} T^{\frac{5}{2}} \tag{40}$$

Specific heat capacity of magnos will be caculated as:

$$C^{magnon} = \frac{\partial U}{\partial T} = \frac{\partial}{\partial T} \sum_k \omega_K < \bar{n}_k >_T \tag{41}$$

$$C^{magnon} = \frac{\partial}{\partial T} \left[0.0456 \left(\frac{1}{2xJSa^2}\right)^{\frac{3}{2}} k_B^{\frac{5}{2}} T^{\frac{5}{2}}\right] \tag{42}$$

$$C^{magnon} = 0.113 \left(\frac{1}{2xJSa^2}\right)^{\frac{3}{2}} k_B^{\frac{5}{2}} T^{\frac{3}{2}} \tag{43}$$

This shows that $C^{magnon} \sim T^{\frac{3}{2}}$

2.3.2. Magnon Heat Capacity in Antiferromagnetism

We have seen that in the absence of an external magnetic field of the two magnon branches are degenerate, i.e

$$\omega_K{}^{\pm} = 2\sqrt{2} Jskxa$$

Hence the internal magnon energy for anti-ferromagnet can be written as:

$$U = \sum_K \omega_K \langle n_k \rangle \tag{44}$$

This can be written as

$$U = \frac{1}{(2\pi)^3} \int_0^{k_{max}} \frac{dk}{exp(\omega_K\beta) - 1} \tag{45}$$

$$U = \frac{1}{(2\pi)^3}\int_0^{k_{max}} \omega_K 4k^2 \frac{dk}{exp(\omega_K\beta)-1} = \frac{1}{2\pi^2}\int_0^{k_{max}} \omega_K k^2 \frac{dk}{exp(\omega_K\beta)-1} \quad (46)$$

$$U = \frac{1}{2\pi^2}\int_0^{k_{max}} 4\sqrt{3}Jsxak^3 \frac{dk}{exp\left(\frac{4\sqrt{3}Jsxak}{k_BT}\right)-1} \quad (47)$$

The upper limit can be taken as infinity for temperature small compared with the Neel temperature. Thus

$$U = \frac{4\sqrt{3}Jsxa}{2\pi^2}\int_0^{\infty} k^3 \frac{dk}{exp\left(\frac{4\sqrt{3}Jsxak}{k_BT}\right)-1} \quad (48)$$

Let $y = \frac{4\sqrt{3}Jsxak}{k_BT}$ and dy $= \frac{4\sqrt{3}Jsxa}{k_BT}dk$, then substituting in to the above equation(2.39),

We get $U = \frac{k_BT}{2\pi^2}\left(k_B\frac{T}{4\sqrt{3}Jsxa}\right)^3\int_0^{\infty} y^3\frac{dy}{e^y-1}$ (49)

But the value of the integral $\int_0^{\infty} y^3\frac{dy}{e^y-1} = \frac{\pi^4}{15}$

Therefore, the internal magnon energy for anti-ferromagnet is

$$U = \frac{\pi^4}{30}\frac{(k_BT)^4}{(4\sqrt{3}Jsxa)^3} \quad (50)$$

Hence the magnon heat capacity is given by:

$$C^{magnon} = \frac{\partial U}{\partial T} = \frac{4\pi^2}{30}\frac{k_B(k_BT)^3}{(4\sqrt{3}Jsxa)^3} \quad (51)$$

Thus the predicted magnon part of the heat capacity is proportional to T^3 which is similar to the Debye phonon heat capacity.

2.4. Ferromagnetic Transition Temperature

Ferromagnetism refers to solids that are magnetized without an applied magnetic field. These solids are said to be spontaneously magnetized. Ferromagnetism occurs when paramagnetic ions in a solid "lock" together in such a way that their magnetic moments all point (on the average) in the same direction. At high enough temperatures, this "locking" breaks down and ferromagnetic materials become paramagnetic. The temperature at which this transition occurs is called the Curie temperature. In the ferromagnetic state at low temperatures, the spins on the various atoms are aligned parallel. There are several other types of ordered magnetic structures. These structures order for the same physical reason that ferromagnetic structures do. The Weiss theory is a mean field theory and is perhaps the simplest way of discussing the appearance of the ferromagnetic state. Thus the basic equation for ferromagnetic materials is

$$M = NS_g\mu_B B_s \quad (52)$$

$$where\ a' = \frac{(\mu_o S_g\mu_B(H+\xi))M}{KT} \quad (53)$$

That is, the basic equations of the molecular field theory are the same as the Para- magnetic case plus the H → H + γM replacement in which for the case of a simple paramagnet:

$M = NS_g\mu_B B_s(a)$ Where B_s is the Brillouin function for spin it is easy to recover the high-temperature results of B_s.

i.e. $B_s(y) = \frac{S+1}{3S}y \ldots\ldots if\ y \ll 1$

where $a = \frac{\mu_o S_g\mu_B H}{KT}$

Let us now indicate how this predicts a phase transition. By a phase transition, we mean that spontaneous magnetization (M ≠ 0 with H = 0) will occur for all temperatures below a certain temperature Tc called the ferromagnetic Curie temperature. At the Curie temperature, for a consistent solution of (51) and (52), we require that the following two equations shall be identical as a′ → 0 and H = 0:

$$M_1 = NS_g\mu_B B_s(a') \quad (54)$$

$$M_2 = \frac{KTa\prime}{NS_g\mu_B B_s\gamma\mu} \text{ with } H \to 0 \quad (55)$$

Where $\mu_B = \frac{eh}{2m}$ is the Bohr magneton, and g is sometimes called simply the g- factor, N is the number of particles per unit volume, If these (equation (53) and equation (54)) are identical, then they must have the same slope as a′ → 0.

That is, we require

$$\left(\frac{dM_1}{da\prime}\right)_{a\prime\to 0} = \left(\frac{dM_2}{da\prime}\right)_{a\prime\to 0} \quad (56)$$

Using the known behavior of $B_s(a')$ ′ as $a' \to 0$ we find that equation (53) gives

$$T_c = \frac{\mu_0 Ng^2 S(S+1)\mu_B{}^2\gamma}{3K} \quad (57)$$

Equation (56) provides the relationship between the Curie temperature T_c and the Weiss molecular field constant γ. Note that, as expected, if γ = 0, then *Tc*=0 (i.e. if γ → 0, there is no phase transition). Further, numerical evaluation shows that if $T \gg T_c$with H =0 have a common solution for M only if M = 0. However, for $T \ll T_c$, numerical evaluation shows that they have a common solution M ≠ 0, corresponding to the spontaneous magnetization that occurs when the molecular field over thermal effects.

The Curie temperature itself is a critical point, where the magnetic susceptibility is theoretically infinite and, although there is no net magnetization, domain-like spin correlations fluctuate at all length scales. The study of ferromagnetic phase transitions, especially via the simplified Ising spin model, had an important impact on the development of statistical physics. There, it was first clearly shown that mean field theory approaches failed to predict the correct behavior at the critical point (which was found to fall under a universality class that includes many other systems, such as liquid-gas transitions), and had to be replaced by renormalization group theory (4). When we vary the external magnetic field H acting on solid its change of magnetization M as a function of temperature T hence the susceptibility χ (T) is given by: $\chi(T) = \lim_{H\to 0}\frac{\partial M}{\partial H}$

Thus the magnetic susceptibility of a solid $\chi(T)$ is

measured and it is used to categorize different kinds of solid like Ferro magnetism in which all magnetic moments are in parallel alignment, the effective ensures the effect of ordering of the system experienced by each atomic site and therefore is given by $H_{eff} = H + \lambda M$ where $\lambda > 0$ is a constant that parameterize the strength of molecular field as a function of the magnetization. Then the mean magnetic moment or magnetization for N atoms is given by

$$M = N\sum_i \mu_i p_i = N\frac{\sum_{-s}^{S}(m_i g\mu_B)e^{-\beta m_i g H_{eff}}}{\sum_{-s}^{s} e^{-\beta g H_{eff}}} \quad (58)$$

$Ng\mu_B B_s(x)$ where $B_s(x)$ is the Brillouin function given by the expression:

$$B_s(x) = \frac{1}{S}\left[\left(S+\frac{1}{2}\right)\coth[\left(S+\frac{1}{2}\right)x] - \frac{1}{2}\coth\frac{x}{2}\right] \quad (59)$$

$$\text{And } x = \frac{g\mu_B H_{eff}}{k_B T}$$

where g is the land factor which depends on the magnitude of L and S foe $x \ll 1$.

$B_s(x) = \frac{(s+1)x}{3}$ and using $H_{eff} = H + \lambda M$ we have a self-consistent equation for M as:

$$M = \frac{Ng^2\mu_B{}^2 S(S+1)(H+\lambda M}{3k_B T}) \quad (60)$$

Then the equation can be written as

$$M\left[1 - \frac{C\lambda}{T}\right] = \left(\frac{C}{T}\right)H \quad (61)$$

but $M = \chi H$ so that the magnetic susceptiblity is given by:

$$\chi = \frac{C}{T - C\lambda} \quad (62)$$

and obtaining the curie W eiss la, $\chi = \frac{C}{T-T_c}$ which is valid for $T \gg T_c$ and which is independent of T and the curie temprature is given by $T_c = C\lambda$

The Curie temperature *TC* is the temperature above which the spontaneous magnetization vanishes it separates the disorder paramagnetic phase at f $T > T_c$ room the ordered ferromagnetic phase at t $T < T_c$ *t*he mean field constant;

$$\lambda = \frac{T_c}{C} = \frac{3k_B T_c}{Ng^2 S(S+1)\mu_B{}^2} \quad (63)$$

Where C is the curie constant. The high temperature susceptibility is generally taken as is evidence for paramagnetic spins.

2.5. Magnetization Reversal for Ferromagnetism

The number of reversal spins is given by the ensemble average of spin wave occupancy number, thus for saturation magnetization with the same assumption for the heat capacity and taking unit volume, the magnetization M (T) as a function of temperature can be computed by nothing that each spin wave mode leads to one spin wave reversal. Thus the spontaneous magnetization at temperature T is given by:

$$M_s = 2\mu_o S_z = 2\mu_o(NS - \sum b_k^+ b_k) \quad (64)$$

$$\text{And } M_s(0) - M_s(T) = -M = 2\mu_o \sum_K < n_k >= \frac{2\mu_o}{(2\pi)^3}\int dk^3 \frac{1}{e^{\frac{Dk^3}{\tau}} - 1}$$

$Where\ M(0) = g\mu_B NS$, which is ground state magnetization or magnetization at absolute zero, ferromagnetic state where all spins can exploit their mutual exchange energy by being preferentially aligned parallel to each other has lower free energy than the state where $H_m = 0$.

Where $D = 2JSx^2$ at low temperature such that $Dk^2{}_{max} \gg \tau$

$$\vartriangle M = \frac{\mu_o}{2}\pi^2\left(\frac{D}{\tau}\right)^{\frac{1}{2}}\int_0^\infty dx x^{\frac{1}{2}}\frac{1}{e^x - 1} \quad (65)$$

Where $\int_0^\infty dx x^{\frac{1}{2}}\frac{1}{e^x-1} = \Gamma\left(\frac{3}{2}\right)\xi(\frac{3}{2}\ 1)$ there fore,

$$\vartriangle M = 0.117\mu_o\left({k_B T}/{D}\right)^{\frac{3}{2}} \quad (66)$$

Thus the reduction in magnetization due to thermal spin wave excitation is

$$\vartriangle M = 0.117\frac{\mu_o}{2a^3}\left({k_B T}/{2Js}\right)^{\frac{3}{2}} \quad (67)$$

We can use the relation of

$$M(T) = M(0)\left(1 - \frac{1}{ns}\right)(0.0587)\left({k_B T}/{2XJSa^2}\right)^{\frac{3}{2}} \quad (68)$$

$$M(T)\Big/_{M(0)} = 1 - (0.0587)\left({k_B T}/{2XJSa^2}\right)^{\frac{3}{2}} \quad (69)$$

Where $n = \frac{N}{V}$ and v is the lattice cell volume $=a^3$:

N is the number of atoms per unit volume that is given by: $N = na^3$.

2.6. Magnetization and Transition Temperature for Anti-ferromagnet

The sub lattice magnetization at temperature T is given by

$$M(T) = g\mu_B \sum_I (S - a_i^+ a_i) \quad (70)$$

Using the spin wave canonical transformation we get the following

$$M(T(= g\mu_B(nS - \sum_k \sinh^2\theta_k - \sum_k < a_k^+ a_k > \cosh 2\theta_k \quad (71)$$

The second term of equation (54) gives the zero-point contribution to the sub lattice spin deviation. It can be shown, on neglecting the Zeeman term, that

$$\vartriangle M_{zeropoint} = g\mu_B \sum_k \sinh^2\theta_k = \frac{1}{2}g\mu_B \sum_k \left\{(1 - \gamma_k{}^2)^{\frac{-1}{2}}\right\} - 1 \quad (72)$$

For a simple cubic lattice this turns out to be $0.078g\mu_B n$. The third term of equation (2.70) gives the temperature dependent part. Taking $M(T) = g\mu_B nS$ which is ground state magnetization and neglecting the second term of equation (2.54) we obtain

$$M(T) = M(0)\left(1 - \frac{1}{nS}\sum_k < n_k > \cosh 2\theta_k\right) = M(0)(1 - \frac{1}{nS}\sum_k \frac{1}{\exp\left(\omega_K/k_BT\right)-1}\cosh 2\theta_k =$$

$$M(0)\left[1 - \frac{1}{nS}\sum_k (1-\gamma_k{}^2)^{\frac{-1}{2}} \frac{1}{\exp\left(\omega_K/k_BT\right)-1}\right]$$

But the value of $(1-\gamma_k{}^2)^{\frac{-1}{2}} = \frac{\sqrt{3}}{ka}$, hence

$$\frac{M(T)}{M(0)} = 1 - \frac{\sqrt{3}}{naS}\sum_k \frac{1}{k\left[\exp\left(\omega_K/k_BT\right)-1\right]} \tag{73}$$

Now the researcher used $\sum_k \frac{1}{k\left[\exp\left(\omega_K/k_BT\right)-1\right]} = \frac{1}{(2\pi)^3}\int_0^{k_{max}} \frac{d^3k}{k\left[\exp\left(\omega_K/k_BT\right)-1\right]}$

The upper limit can be taken as infinity for temperatures small compared with the Neel temperature. Thus

$$\sum_k \frac{1}{k\left[\exp\left(\omega_K/k_BT\right)-1\right]} = \frac{1}{(2\pi)^3}\int_0^{\infty} \frac{4k^2dk}{k\left[\exp\left(\omega_K/k_BT\right)-1\right]} = \frac{1}{2\pi^2}\int_0^{\infty} \frac{kdk}{exp\left(\frac{4\sqrt{3}Jsxak}{k_BT}\right)-1}$$

$$let\ y = \frac{4\sqrt{3}Jsxak}{k_BT}; k = \frac{k_BT}{4\sqrt{3}Jsxak}y \text{ and } dk = \frac{k_BT}{4\sqrt{3}Jsxak}dy$$

$$\sum_k \frac{1}{k\left[\exp\left(\omega_K/k_BT\right)-1\right]} = \frac{1}{2\pi^2}\left(\frac{k_BT}{4\sqrt{3}Jsxak}\right)^2\int_0^{\infty} \frac{ydy}{e^y-1}$$

The value of the integration $\int_0^{\infty} \frac{ydy}{e^y-1} = \frac{\pi^2}{6}$

Hence substituting all these values in equation (2.56) we will get

$$\frac{M(T)}{M(0)} = 1 - \frac{\sqrt{3}}{12NS}\left(\frac{k_BT}{4\sqrt{3}Jsxak}\right)^2 \tag{74}$$

But when $\frac{M(T)}{M(0)}$ goes to zero, T approaches to T_N which gives

$$T_N = (48)^{\frac{3}{4}}\left(\frac{JS}{K_B}\right)(NS)^{\frac{1}{2}}x \tag{75}$$

3. Results and Discussion

In the previous chapter we have obtained expressions of magnetization, specific heat and transition temperature for antiferromagnetic magnons based on spin wave theory using the Holstein-Primakoff transformations. In addition to these we have also calculated the number of magnons excited in the mode k at a temperature T using Green's function. To calculate all of the above quantities first we have got the dispersion relation for magnons in an anti-ferromagnet and ferromagnet. The dispersion relation for magnons in an Antiferromagnete is linear in k which is quite different from that of magnons in a ferromagnet which is quadratic in k.

In this chapter we tried to generalize the main results obtained in this work and investigate the results with the help of figures.

3.1. Effects of Temperature on Magnetization

The reduced magnetization as a function of temperature can be computed by noting that each spin-wave mode leads to one spin reversal distributed coherently throughout the entire lattice. We have got the theoretical formalism describing the dependence of reduced magnetization due to thermal spin-wave excitations on temperature as follows:

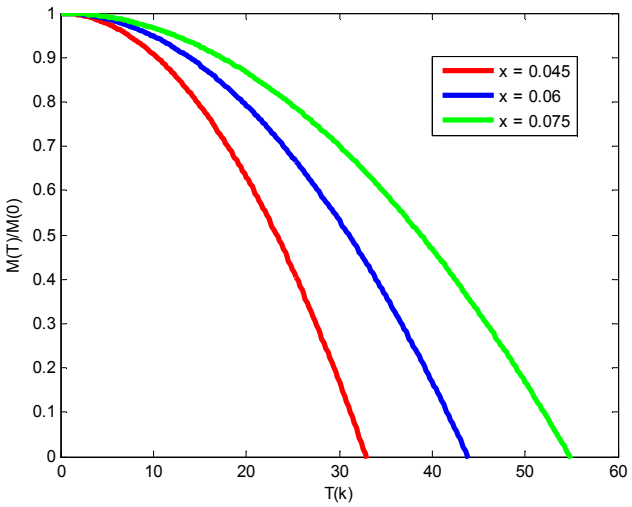

Figure 1. *Reduced magnetization VS temperature when values of x are kept constant.*

As we have seen from the figure Curves are slightly different for different values of the concentration (x) of the manganese ion, however, they all have a convex upward shape. The reduced magnetization versus temperature curve is obtained for x = 0.045, 0.06 and 0.075. In a reduced magnetization, versus reduced temperature graph, the reduced magnetization decreases and goes to zero with increasing reduced temperature. At T < Tc there is saturation magnetization (ferromagnetic state) and at T > Tc there is a Paramagnetic region.

As $\frac{M(T)}{M(0)} \to 0$ then $T \to T_c$ this gives, $T_c = \chi\left(\frac{2JS}{K_B}\right)\left(\frac{na^3S}{0.0587}\right)2^{\frac{2}{3}}$, thus there exists the possibility of ferromagnet below a certain critical temperature *Tc* called the curie temperature which is directly proportional to the concentration of the impurity atom $T_c \approx \chi$

However, for $T \ll T_c$, numerical evaluation shows that they have a common solution M ≠ 0, corresponding to the spontaneous magnetization that occurs when the molecular field over thermal effects. The Curie temperature itself is a critical point, where the magnetic susceptibility is theoretically infinite and, although there is no net magnetization, domain-like spin correlations fluctuate at all length scales. The study of ferromagnetic phase transitions, especially via the simplified Ising spin model, had an important impact on the development of statistical physics. Thus, there exists the possibility of ferromagnetism below a certain Critical temperature Tc called the Curie temperature which is directly proportional to the concentration of the impurity atom. i.e. T_c is proportional to the concentration (x): At temperature below Tc, the ferromagnetic state is stable. For; $T \to 0$ the magnetic moment when all spins are aligned completely parallel. As we have seen from the figure 2, the graph of Neel temperature versus manganese ion concentration is linear. The dependence of Neel temperature on concentration is observed for GaMnN for the range (0.2- 0.8). The figure below shows that the Neel temperature for GaMnN increases linearly with increasing the concentration of manganese ion increases in the range given above from the equation(3.58) and taking the constants for GaMnN *TN*=731.5 *x* thus for our calculation the highest Neel temperature obtained T=146.3k within the concentration of 0.2 as shown in the figure below.

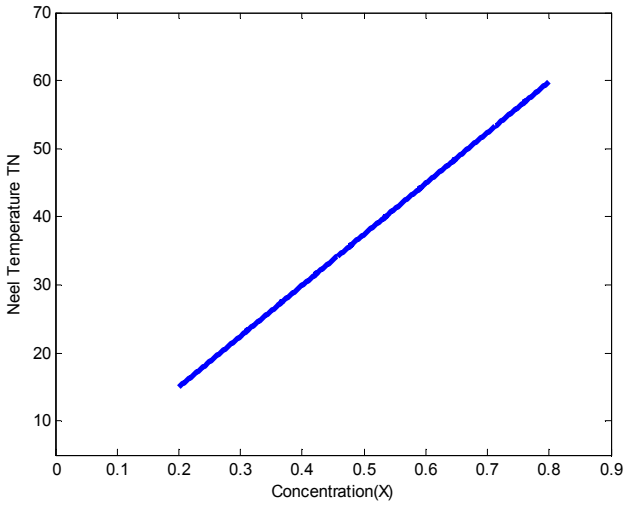

Figure 2. *Neel temperature versus concentration.*

3.2. Implication of Specific Heat on Temperature

The detailed ferromagnetic and antiferromagnetic magnon specific heat capacity per unit volume versus temperature T for GaMnN will be shown in this work. To derive the specific heat we neglect magnon-magnon interactions, which is justifiable in the very-low-temperature regions. We have seen that magnons behave like Bose particles. Thus the internal energy of a system of magnons in thermal equilibrium at temperature T using equation(3.35) is given by: $U = \frac{\pi^4}{30}\frac{(k_BT)^4}{(4\sqrt{3}Jsxa)^3}$

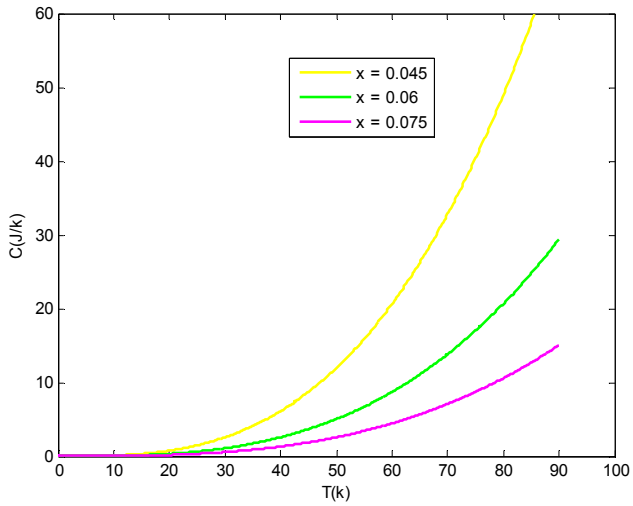

Figure 3. *Heat capacity per unit volume VS temperature when values of x are kept constant.*

Taking the derivative of the above equation with respect to T, we get the specific heat capacity per unit volume, which is $C^{magnon} = \frac{4\pi^2}{30}\frac{k_B(k_BT)^3}{(4\sqrt{3}Jsxa)^3} \Rightarrow$ Magnon heat capacity of antiferromagnetic

Because U goes to zero just at T_N and vanishes at all temperatures above it, there is no latent heat associated with the disappearance of the magnetization (5). Thus the heat capacity for anti-ferromagnet in the low-temperature region arising mainly from magnons is proportional to T^3 and using equation (2.27), we can find the magnon heat capacity for ferromagnetic.

$Hence, C^{magnon} = 0.113\left(\frac{1}{2xJSa^2}\right)^{\frac{3}{2}}k_B^{\frac{5}{2}}T^{\frac{3}{2}} \Rightarrow$ Magnon heat capacity for ferromagnet.

Then, we can draw the graph that shows the result of heat capacity per unit volume VS temperature when values of x are kept constant for ferromagnet in the figure that is shown below.

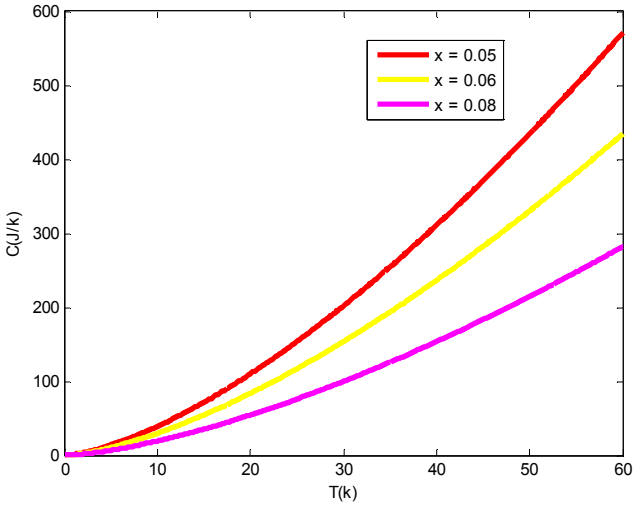

Figure 4. *Heat capacity per unit volume VS temperature when values of x are kept constant in ferromagnet.*

Table 1. *Summary of spin wave properties (at low energy and at low temperature).*

	Dispersion relation	Magnetization	Magnetic Specific Heat
Ferromagnet	$\omega = A_1 K^2$	$\approx T^{\frac{3}{2}}$	$\approx T^{\frac{3}{2}}$
Antiferromagnete	$\omega = A_1 K$	$\approx T^2$	$\approx T^3$

4. Conclusion

In the present investigation we have studied the ferromagnetism and anti-ferromagnetism of GaN which is doped with transition metal element *(manganese). $Ga_{1-X}Mn_XN$* as can be considered as a model system for III-V diluted magnetic semiconductors, which are promising materials for future spintronics applications. In view of future applications, a proper characterization and understanding of the physical properties of $Ga_{1-X}Mn_XN$ is essential, and techniques to increase the ferromagnetic transition temperature like post-growth annealing must be explored. While dilute magnetic semiconductors could be a useful class of materials and assume a crucial role in enabling the semiconductor spintronics devices, much remains unanswered with regards to the mechanism of magnetism in these materials. Traditional III-V candidates such as $Ga_{1-X}Mn_XN$, which are typically p-type, have been studied in great detail. Optical as well as electrical measurements have established carrier-mediated ferromagnetism in these materials. However, the highest *Tc* obtained in these materials >300K, making them undesirable for technological applications and from magnon distribution function, the total number of magnons in all modes excited at temperature T can be calculated as:

$\sum_k n_k = (0.0587)\left(\frac{k_B T}{2XJSa^2}\right)^{\frac{3}{2}}$, Which follows $T^{\frac{3}{2}}$ relation and the Neel temperature for $Ga_{1-X}Mn_XN$ increases when the concentration of manganese ion increases in the range $0.2 \leq x \leq 0.8$ hence $Ga_{1-X}Mn_XN$ is found to be anti-ferromagnetism in the Neel temperature of $T_N = 146.3 - 585.2$ and thus for our calculation the highest Neel temperature obtained T=146.3k within the concentration of 0.2. The heat capacity for anti-ferromagnet in the low temperature region arising from magnons is proportional to T^3 which is similar to the Debye phonon heat capacity whereas the heat capacity of ferromagnet is proportional to $T^{\frac{3}{2}}$ and the specific heat decreases with concentration keeping the temperature constant $that\ is\ C^{magnon} \approx \frac{1}{x^3}$, the magnetization reversal is flew the relation of $\approx T^{\frac{3}{2}}$ and $\approx T^2$ respectively for ferromagnetic and anti ferromagnetic but vanishes as $T \to T_c$ for ferromagnetism and $T \to T_N$ for antiferromagnetism.

References

[1] Gerald, Thaler, JR. 2004, phd dessertation. Development of Gallium Nitridebased Dilute Magnetic Semiconductors for Magneto-Optical Applications.

[2] Yosida. Theory of Magnetism. Berlin: Springe, 1996.

[3] Raebigr, Hannes. 2006, Ferromagnetism in (Ga,Mn) As AND (Ga,Mn)N, Auditorium E.

[4] "Introduction to the magnetic properties of solids". Chakravarty A. S. 1980, Saha Institute of Nuclear Physics.

[5] Daniel, C. Mattis. The theory of magnetism. New York: s.n., 1965.

[6] Electronic Structure and Optical Properties of Semiconductors. Matioli etla. 2009, Journal of Applied Physics.

[7] Spintronics And Ferromagnetism In Wide-Band-Gap. Dietl et al. 2000, Semiconductor Spintronics Project of Japan Science.

[8] Nakamura, M. Senoh, S. Nagahma, N. Iwasa, T. Yamada, T. Matsuahita, H. Kiyoku, and Y. Sugimoto,. 1996, Jpn. J. Appl. Phys. pp. 35, 174.

[9] Optical properties of Mn-doped GaN. Boukortt. 2012, PHYSICAL REVIEW B, pp. 85, 033302.

[10] Optical properties of III-Mn-V ferromagnetic semiconductors. Burch, D. D. Awschalom, D. N. Basov. 2008, Journal of Magnetism and Magnetic Materials, pp. 1-4.

[11] Mydosh. An experimental Introduction in Spin Glasses. 1993.

[12] Zinc Oxide based Diluted Magnetic Semiconductor. Shivaraman, Ramachandran. 2006, phd dessertation.

[13] Federick, R. Fundamentals of STATISTICAL AND THERMAL Physics, International Edition". Singapore. 1985.

[14] Gil. Group III Nitride Semiconductor Compounds. Oxford University Press, England, s.n., 1998.

[15] High Brightness Violet InGaN/GaN Light Emitting Diodes. Wierer et al, Nakamura and Faso. 2004, 1999, Journal of Applied Physics.

[16] Farah, A. D. *Ga1−xMnxN* Magnetic Semiconductors: First-Principles Study. the degree of Master of Science in Physics. 2008.

[17] Recent progress towards the development of ferromagneticnitride semiconductors for spintronic applications. Newman. 2006., phys. stat. sol. (a) 203, 2729– 2737.